International Journal of Chemical, Materials and Biomolecular Sciences
ISSN: 2415-6620
Vol:5, No:11, 2011

Hydrolysis Characteristics of Polycrystalline Lithium Hydride Powders and Sintered Bulk

M. B. Shuai, S. Xiao, Q. S. Li, M. F. Chu, X. F. Yang

***Abstract*—**Ambient hydrolysis products in moist air and hydrolysis kinetics in argon with humidity of RH1.5% for polycrystalline LiH powders and sintered bulks were investigated by X-ray diffraction, Raman spectroscopy and gravimetry. The results showed that the hydrolysis products made up a layered structure of $LiOH•H_2O/LiOH/Li_2O$ from surface of the sample to inside. In low humid argon atmosphere, the primary hydrolysis product was Li_2O rather than LiOH. The hydrolysis kinetic curves of LiH bulks present a paralinear shape, which could be explained by the "Layer Diffusion Control" model. While a three-stage hydrolysis kinetic profile was observed for LiH powders under the same experimental conditions. The first two sections were similar to that of the bulk samples, and the third section also presents a linear reaction kinetics but with a smaller reaction rate compared to the second section because of a larger exothermic effect for the hydrolysis reaction of LiH powder.

***Keywords*—**Hydrolysis, lithium compound, polycrystalline lithium hydride

I. Introduction

LITHIUM hydride (LiH) has many applications [1]-[3], such as a precursor in chemical synthesis (in particular for lithium aluminum hydride and lithium borohydride), both a coolant and shielding in nuclear reactors, and as the fusion fuel in thermonuclear weapons, in the deuteride form. But LiH is a strong reducing agent; it may react exothermically with water to form caustic lithium hydroxide (LiOH) and hydrogen gas, and may ignite spontaneously in moist air, particularly when powdered. Therefore, LiH must be stored and handling in low humidity atmosphere, which makes its very important to clarify the reaction characteristics of LiH mass or powders with water in low humid atmosphere. Many studies on the hydrolysis of single crystal and polycrystalline LiH have been carried out under differential experimental conditions [4]-[8]. Researchers from Oak Ridge Y-12 Plant had studied the surface reaction products of single crystal and polycrystalline LiH with water vapour twenty years before [4], [5]. In recent years, researchers, such as Tanski [6] , Balooch [7] , Haertling [8], [9] and Wilson [10], etc., carried out further studies on the hydrolysis kinetics and its mechanisms of LiH. The phase diagram of $Li\text{-}H_2O$ was amended by Balooch *at al.* [7], which demonstrated very well all the possible hydrolysis products. The trilayer model introduced by McLaughlin *et al.*[4] was generally accepted as a composition profile for LiH hydrolysis.

The authors are all with the China Academy of Engineering Physics; P. O. Box 919-71, Mianyang, Sichuan, 621900 China (corresponding author is Mao-Bing Shuai, phone: +86 13981103553; e-mail: shuaimb@ sina.com).

According to the phase diagram and the trilayer model, the hydrolysis products of LiH are LiOH and H_2 under ambient conditions with water vapor partial pressure of less than approximately 500 Pa (RH15%), and the product of $LiOH•H_2O$ will appear under higher humidity. There have theoretic [7] and experimental [5], [6], [11] evidences to illustrate the existence of Li_2O as a layer between the base LiH and the LiOH. Haertling et al [8], [9] introduced a model named "Layer Diffusion Control", which explained very well the 'paralinear' behavior and the mechanisms of LiH hydrolysis. Although these studies depicted in great detail the hydrolysis behavior of LiH in various conditions of temperature and humidity, there still lack straight observations for the occurring of Li_2O during hydrolysis process of LiH. Moreover, it is also very important to know this process in order to control the hydrolysis in the practical process of the LiH component fabrications.

The ambient hydrolysis products in moist air and the hydrolysis kinetics in argon with humidity of RH1.5% for polycrystalline LiH powders and sintered bulks were investigated by X-ray diffraction, Raman spectroscopy and gravimetry.

II. Experimental

A. Materials and Sample Preparation

LiH was obtained with the pyro-reaction of metal lithium and high purity hydrogen gas, following with a mechanical crushing process for the cooled melt and then sieved with standard sieve of 20, 40, 60 and 100 meshes. The nominal particle size was 850, 355, 250, and 150 μm, respectively. Polycrystalline LiH bulk samples were prepared by powder metallurgy. The powders with nominal size of 150 μm were cold isostatic pressed and sintered at approximately 520℃ to obtain a consolidated bulk with density of 0.76 g/cm^3. The bulk samples were machined to the size of 20 mm diameter, 10 mm high and the surface was polished using metallographic SiC sand paper with powder size of 19 μm to clear the surface corrosion products. The samples for Raman and XRD analyses were sealed in a chamber made from stainless steel. There is a window on the top of the chamber, which is adapted as a function of Raman or XRD device. A transparent glass window was used for Raman measurements and it was replaced by a mylar window for the XRD analyses. All samples' handling and preparation were performed in a glove box filled with nominally dry argon (approximately less than 10 ppm of H_2O).

B. Equipment and Analyzing Procedure

Gravimetry was carried out at 25 ℃ by monitoring the weight gain during the exposure time using an electronic balance with a precision of 0.01 mg in the same glove box where the samples were prepared. The water concentration and the total pressure in the glovebox were monitored instantly and adjusted by a controlling system. During the entire exposure, the total pressure was maintained at a few hundred Pascals higher than atmospheric pressure to decrease the possible gaseous contamination of outer gases penetrating into the glove box. A sample mass of approximately 5 g of LiH powders for each gravimetric measurement were used. The weight was recorded every 5 min for the first hour, and the interval was extended to 10-20 min during the following exposure time.

Raman spectra were collected using an Almega XR Dispersive Raman spectroscope (Thermo Fisher Scientific Co., USA). The laser power on the samples was 20 mW with the wavelength of 532 nm. A total of 20 scans per spectrum were continuously recorded and the resolution of the spectrometer was 2 cm^{-1}. The surface morphologies of the sample were detected using GX71 metallographic microscope (German Olympus Company). XRD experiments were performed using X Pert PRO with voltage of 35 kV and scan angle of 15.0-50 degrees.

III. Results and Discussion

A. The corrosion products of polycrystalline LiH bulk under humid air

The corrosion products of polycrystalline lithium hydride under humid air (RH60%±2%) at ambient temperature were detected using X-ray diffraction, which was showed in Fig.1.

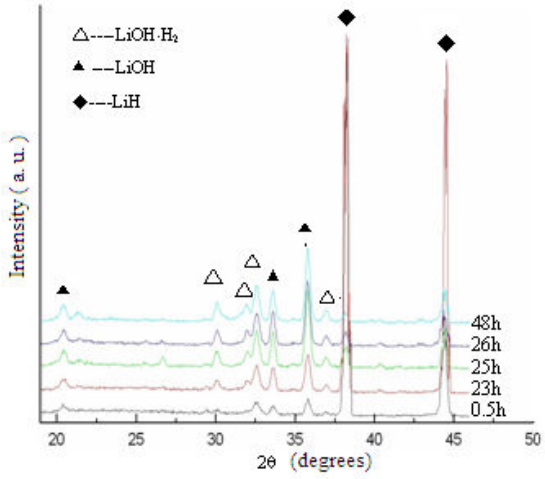

Fig. 1 Evolution versus time of XRD pattern of polycrystalline LiH bulk exposure to air with humidity of RH60% at room temperature

As can be seen from Fig.1, the integrated intensities for each product changed with the exposure time. The integrated intensities of LiH XRD peaks decreased gradually whereas the integrated intensities of LiOH and $LiOH·H_2O$ XRD peaks increased gradually with the increasing of the exposure time, which revealed that the amount of corrosion products of LiH increased with the exposure time. This can also be showed in Raman spectra in Fig.2 for the bulk samples exposed in air with humid of RH60% at ambient temperature. The product of Li_2CO_3 can be detected using this method, which was the result of the reaction of LiOH and CO_2 in air. The detected Raman intensities of Li_2O almost had no change during the entire exposure time, as showed in Fig.2. Fig.3 showed the depth profile of the products for the bulk sample exposed in air with humid of RH60% at temperature of 25℃. It can be seen that the product of Li_2O located more inner than LiOH, which may imply that Li_2O located between the hydrolysis product of LiOH and the LiH base.

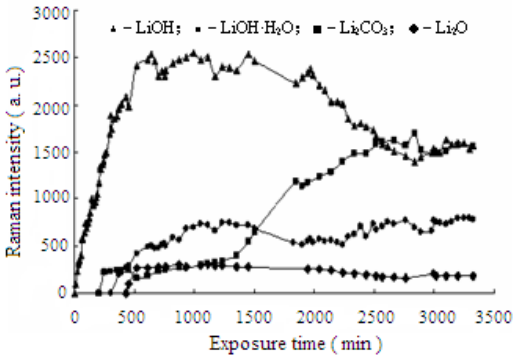

Fig. 2 Exposure time dependence of Raman intensities of hydrolysis products for polycrystalline LiH bulk exposure in ambient air with humidity of RH60%

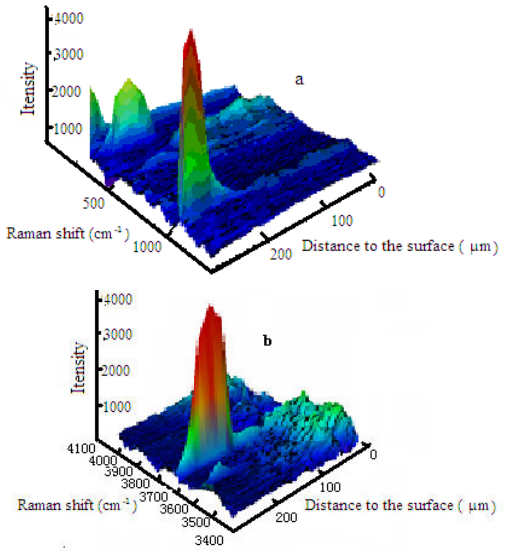

Fig. 3 Depth profile of the hydrolysis products: (a) Li_2O and Li_2CO_3; (b) LiOH and $LiOH·H_2O$ for polycrystalline LiH bulk exposure in humid air at temperature of 25℃

Atmosphere humid has obvious effect on the content of the hydrolysis products of LiH as showed in Raman spectra in Fig.4. The larger the humidity, the higher the hydrolysis rate of

LiH. LiOH and Li_2O were detected even in dry argon atmosphere because of the trace moisture impurity in argon or the absorbed water in the system.

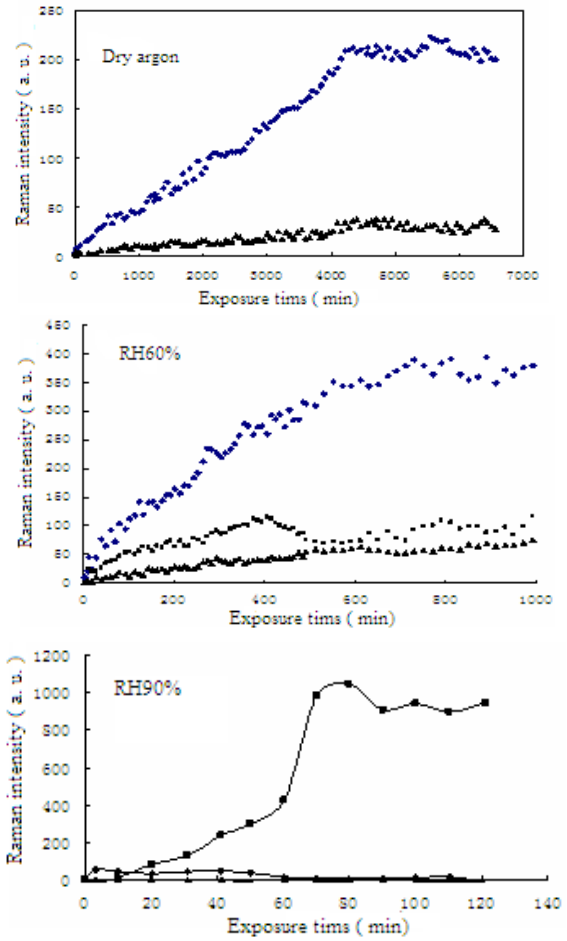

Fig. 4 Raman intensities versus time for hydrolysis products of polycrystalline LiH bulk exposure in argon with different humidities. In figures, "□" denotes the product of LiOH, "▲" denotes Li_2O, and "■" denotes $LiOH·H_2O$

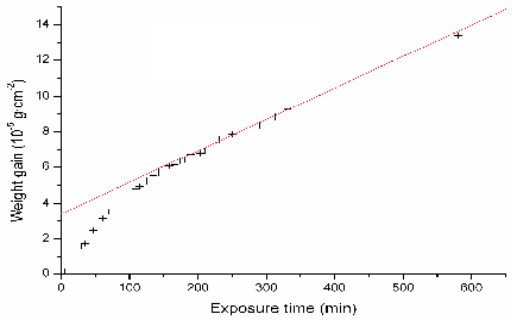

Fig. 5 Weight gain versus time for polycrystalline LiH bulk exposure in ambient argon with humidity of RH1.5% (the linear fitting of the second section data of the kinetics was also showed)

B. The hydrolysis products and kinetics of polycrystalline LiH bulk under low humid argon

The Li_2O can be detected for LiH exposure even in relatively dry argon as showed in Fig.4 and this product is likely located between the hydrolysis product of LiOH and the LiH base as deduced from Fig.3. We need to make sure, at which stage does the Li_2O occur during the hydrolysis process and what effect will it has on the hydrolysis kinetics. Figure 5 showed the weight gain versus the exposure time for polycrystalline LiH bulk exposure in argon with RH1.5% at 25□. As can be seen that the weight gain starts with a high rate, but slows down gradually in the first stage of about 160 min and grows at a constant rate in the second stage. The gravimetric data were consistent well with references [7], [11], [12] on LiH hydrolysis, all of which presented such a 'paralinear' behavior of hydrolysis rates in spite of different experimental methods and the states of the samples used in these studies.

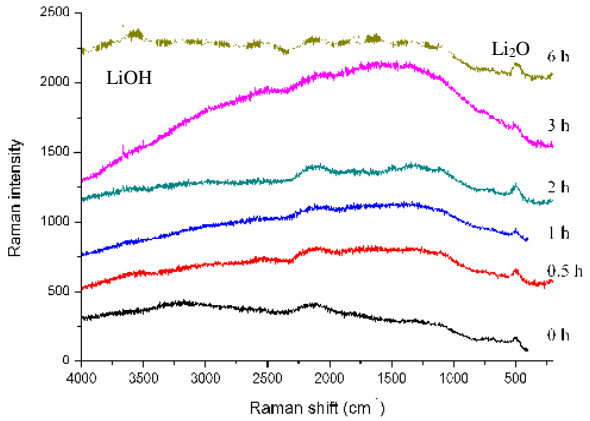

Fig. 6 Evolution versus time of Raman spectra of polycrystalline LiH bulk exposuring in ambient argon with humidity of RH1.5%

The relationship between the 'paralinear' hydrolysis rates and the corresponding reactions was interpreted by 'Layer Diffusion Control' model in [9], of which the core idea was that the diffusion in Li_2O layer determined the overall hydrolysis rate and the thickness of Li_2O layer acted as the key factor. According to the model, Li_2O is the product formed in the parabola-like stage and goes thicker and deeper inside the sample with the exposure time, resulting in a decreasing of the hydrolysis rate; whereas in the linear stage two reactions simultaneously occur at both sides of Li_2O layer and Li_2O is both produced and consumed at the same rate, resulting in a steady Li_2O thickness and a consequent stable hydrolysis rate. The Raman spectra coordinated well with the model, as showed in Fig.6. A sharp Raman shift at near 3654 cm^{-1} and a broadly one at range of 500-520 cm^{-1} were observed obviously during the whole exposure period for LiH bulk sample in argon with humidity of RH1.5%. Raman shift at 3654 cm^{-1} attributes to the stretching vibration of O-H bond in LiOH and the one at 500-520 cm^{-1} to the product of Li_2O [13], [14]. Li_2O can be detected during the whole exposure time of this study, and after approximately three hours exposure can LiOH be detected by

Raman spectroscopy. This may imply that in such atmosphere, the primary product of LiH hydrolysis is Li_2O, rather than LiOH, which provides experimental evidence to the 'Layer Diffusion Control' model for the hydrolysis kinetics of LiH. Moreover, the fact that Li_2O can be detected even for the fresh sample illustrates that LiH can react quickly with water to produce Li_2O even in relatively low humid atmosphere with humidity of RH1.5%.

Data for LiH hydrolysis kinetics and the thickness of Li_2O layer at different water concentrations were reported in another report [15].

C. Hydrolysis products and kinetics of LiH powders exposure to humid argon

The powder morphologies before and after hydrolysis were showed in Fig.7. The particles have various morphologies, such as cubic, clubbed, sheet, and acetabuliform etc. Hydrolysis reaction occurs preferably at the superfine particles adsorbed on the crystals and the uneven surface of crystals. The Raman spectra were also collected for LiH powders under humid argon, which were showed in Fig.8. It can be seen that the product of Li_2O occurred at the same stage as the bulk samples as shown in Fig.6. That is to say, the preliminary hydrolysis product was Li_2O at the first stage of hydrolysis, and a few minutes later could the product of LiOH be detected using Raman spectroscopy for LiH hydrolysis under low humid atmosphere.

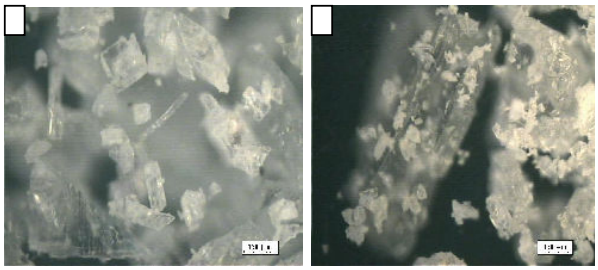

Fig. 7 SEM images of LiH powders, (a) before, and (b) after hydrolysis in low humid argon

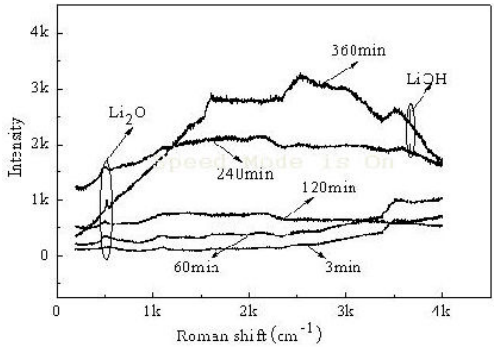

Fig. 8 Ambient Raman spectra of hydrolysis products for LiH powders with particle size of less than 850 μm in RH1.5% argon

In order to know whether the LiH powders have the same hydrolysis kinetics and the product of Li_2O has the same effect on it as bulk samples, the weight gain dependence with the exposure time was obtained by gravimetric method, which was showed in Fig.9. The curves in Fig. 9 have similar shape for different particle size. Nevertheless, the particle radius has obvoius effect on the hydrolysis rate: the larger the paticles, the bigger the weight gain during the same exposure time. Maupoix, *et al*. got a similar conclusion in their study [16]. All kinetics curves exhibit a three stage shape, which were different with those for bulk samples as showed in Fig.5. The first two stages were similar to those of bulk samples: an initial parabola-like stage followed by a linear one, which implied that Li_2O had the same effect on the hydrolysis kinetics. But the third stage was observed several hundred minutes later of exposure for powder samples with the paticle size of less than 850 μm. This stage had a smaller reaction rate, possibly because of the thermal effect of the hydrolysis reaction. The LiH hydrolysis reaction is exothermal. Compared with the bulk samples, the powders have more surface areas and larger reaction rate, resulting in larger amount of exothermal. The accumulated heat will increase the temperature of particles and decrease the hydrolysis reaction rate [7]. In low humid atmosphere, hydrolysis occurs only in surface lamella of the bulk sample, therefore, smaller quantity of heat will release and the effect of the accumulated heat on the hydrolysis kinetics can not be detected in this study.

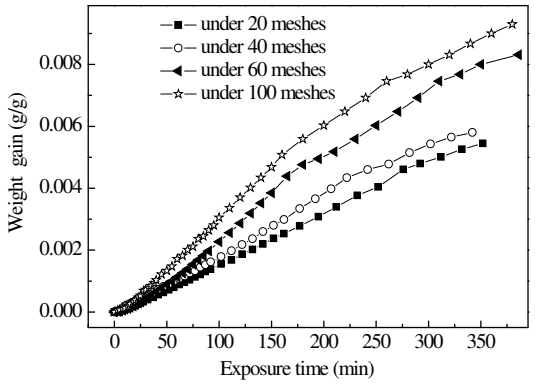

Fig. 9 Ambient hydrolysis kinetics for LiH powders with different particle size in argon with humidity of RH1.5%

IV. Conclusions

The hydrolysis products of polycrystalline LiH make up a layered structure of $LiOH{\cdot}H_2O$ / LiOH / Li_2O from the surface to the inside of the sample.The primary hydrolysis product of LiH in low humid argon was Li_2O rather than LiOH, and there needed a long time to observe the products of LiOH and $LiOH{\cdot}H_2O$. For example, after three and six hours could LiOH and $LiOH{\cdot}H_2O$ be detected, respectively, by Raman spectroscopy in argon with humidity of RH15%. The hydrolysis kinetic curves of LiH bulk present a paralinear shape, which was a combination of a parabolic section and a linear section. This was attributed to two different reaction stages as explained by

the "Layer Diffusion Control" model. While a three-stage hydrolysis kinetics profile was observed for the lithium hydride powders samples. The first two sections were similar to that of the bulk samples, and the third section also present a linear reaction kinetics but with a lower reaction rate compared with the second section, because of the larger exothermic effect for the hydrolysis reaction of lithium hydride powder.

ACKNOWLEDGMENT

The authors would like to thank all the contributors, especially Luo Li-zhu, Jiang Chun-li, and Tan Shi-yong from Science and Technology on Surface Physics and Chemistry Laboratory for their analyzing works. And Xian Xiao-bin, Yang Wei-cai from China Academy of Engineering Physics for their discussions.

REFERENCES

[1] Peter J. Turchi, *Propulsion techniques: action and reaction*. AIAA, ISBN978-1-56347-115-5, 1998, PP.339-341.
[2] M. Olszewski, M. Siman-Tov, "Development of Encapsulated Lithium Hydride Thermal Energy Storage," *Oak Ridge National Lab. Report*. CONF-890815-1 (DE89 010169), 1989.
[3] J. Lu, Z. Z. Fang, H. Y. Sohn, "A hybrid method for hydrogen storage and generation from water," *Journal of Power Sources*, vol. 172, no. 2, pp. 853-858, 2007.
[4] J. F. McLaughlin, S S.Cristy, "Composition of corrosion films on lithium hydride surfaces after exposure to air," *Oak Ridge Y-12 Plant Report*, Y-1929, Oak Ridge, TN, 1974.
[5] S. S. Cristy, "SIMS depth profiling of an insulating air-sensitive material," *Oak Ridge Y-12 Plant Report*, Y/DW-725, Oak Ridge Y-12 Plant, 1987.
[6] J. Tanski, "Analysis of a new reaction mechanism for hydrolysis of LiH," *Los Alamos National Laboratory Report*, LAUR-00-5324, Los Alamos National Laboratory, 2000.
[7] M. Balooch, L. Dinh, D. Calef, "The reaction kinetics of lithium salt with water vapor," *J. Nucl. Mater.*, vol. 303, no. 2-3, pp. 200-209, 2002.
[8] C. L. Haertling, R. J. Hanrahan, R. Smith, "A literature review of reactions and kinetics of lithium hydride hydrolysis," *J. Nucl. Mater.*, vol. 349, pp. 195-233, 2006.
[9] C. L. Haertling, R. J. Hanrahan, J. R. Tesmer, "Hydrolysis studies of polycrystalline lithium hydride," *J Phys Chem C*, vol. 111, no. 4, pp.1716-1724, 2007.
[10] K. V. Wilson, B. M. Patterson, J. Phillips, "Microbalance study of the corrosion kinetics of lithium hydride by water," *J. Nucl. Mater.*, vol. 374, pp. 229-240, 2008.
[11] R.P. Awbery, D.A. Broughton, S.C. Tsang, "In situ observation of lithium hydride hydrolysis by DRIFT spectroscopy," *J. Nucl. Mater.*, vol. 373, pp. 94-102, 2008.
[12] G. L. Powell, "The Spectropus System: Remote Sampling Accessories for Reflectance, Emission, and Transmission Analysis Using Fourier Transform Infrared Spectroscopy," *Appl. Spectrosc.,* vol. 46, no. 1, pp. 111-125, 1992.
[13] T. Osaka, I. Shindo, "Infrared reflectivity and Raman scattering of lithium oxide single crystals," *Solid State Communications*, vol. 51, no. 6, pp.421-424, 1984.
[14] Y. Ishii, T. Nagasaki, "Temperature dependence of the Raman spectrum in lithium oxide single crystal," *J. Am. Ceram. Soc.*, vol. 74, pp. 2324-2326, 1991.
[15] Sa Xiao, Mao-bing Shuai, Ming-fu Chu, Qi-shou Li, Huo-gen Huang, "Li_2O thickness and water concentration effects on LiH hydrolysis kinetics by gravimetry and Raman spectroscopy," *J. Nucl. Mater.* Submitted for publication.
[16] C. Maupoix, J. L. Houzelot, E. Sciora, G. Gaillard, S. Charton, L. Saviot, F. Bernard, "Experimental investigation of the grain size dependence of the hydrolysis of LiH powder," Powder Technology, vol. 208, pp. 318-323, 2011.